

Automatic brain tumor segmentation in 2D intra-operative ultrasound images using MRI tumor annotations

Mathilde Gajda Faanes^{1,2*}, Ragnhild Holden Helland^{1,3},
Ole Solheim^{4,5}, Ingerid Reinertsen^{1,3}

¹*Department of Health Research, SINTEF Digital, Trondheim, Norway.

²Department of Physics, Norwegian University of Science and
Technology (NTNU), Trondheim, Norway.

³Department of Circulation and Medical Imaging, Norwegian University
of Science and Technology (NTNU), Trondheim, Norway.

⁴Department of Neurosurgery, St. Olavs hospital, Trondheim, Norway.

⁵Department of Neuromedicine and Movement Science, Norwegian
University of Science and Technology (NTNU), Trondheim, Norway.

*Corresponding author(s). E-mail(s): mathilde.faanes@sintef.no;

Abstract

Purpose: Automatic segmentation of brain tumors in intra-operative ultrasound (iUS) images could facilitate localization of tumor tissue during resection surgery. The lack of large annotated datasets limits the current models performances. In this paper, we investigate the use of tumor annotations in pre-operative MRI images, which are more easily accessible than annotations in iUS images, for training of deep learning models for iUS brain tumor segmentation.

Methods: We used 180 annotated pre-operative MRI images with corresponding unannotated iUS images, and 29 annotated iUS images. Image registration was performed to transfer the MRI annotations to the corresponding iUS images before training models with the nnU-Net framework. To validate the use of MRI labels, the models were compared to a model trained with only US annotated tumors, and a model with both US and MRI annotated tumors. In addition, the results were compared to annotations validated by an expert neurosurgeon on the same test set to measure inter-observer variability.

Results: The results showed similar performance for a model trained with only MRI annotated tumors, compared to a model trained with only US annotated tumors. The model trained using both modalities obtained slightly better results

with an average Dice score of 0.62, where external expert annotations achieved a score of 0.67. The results also showed that the deep learning models were comparable to expert annotation for larger tumors ($> 200 \text{ mm}^2$), but perform clearly worse for smaller tumors ($< 200 \text{ mm}^2$).

Conclusion: MRI tumor annotations can be used as a substitute for US tumor annotations to train a deep learning model for automatic brain tumor segmentation in intra-operative ultrasound images. Small tumors is a limitation for the current models and will be the focus of future work. The main models are available here: https://github.com/mathildefaanes/us_brain_tumor_segmentation/tree/main.

Keywords: Ultrasound, Segmentation, Brain tumors, Deep learning

Introduction

The most frequent group of primary brain tumors are gliomas arising from glial cells. Gliomas are categorized into subtypes based on histopathological characteristics and molecular markers associated with their aggressiveness [19]. The tumor cells tend to infiltrate the normal brain tissue, creating a diffuse border and making them largely incurable [8]. However, treatment can prolong life and improve or at least prolong quality of life and brain functions [18]. Surgical resection is often the preferred primary treatment option, where studies have shown that the extent of tumor resection is linked to prolonged survival [13, 23]. Nevertheless, removing healthy surrounding tissue in this process could impact the function of the patient negatively [24]. Precise localization of the tumor border is therefore crucial for a successful surgery.

During surgery, pre-operative MRI (pMRI) images are often used in a neuronavigation system, where the images are registered to the patients position on the operating table. An optically tracked tool, such as a pointer, can be used so that the surgeon can see the corresponding position of the pointer on the patient and the pMRI images during surgery. However, due to inaccuracies in the pMRI-to-patient registration and subsequent brain shift, the position of the pointer shown on the pMRI images cannot be fully trusted. Brain shift refers to tissue displacements due to pressure changes, edema, resection or other factors resulting in a mismatch between the image and the real position of the patient [12]. Intra-operative ultrasound imaging (iUS) can be used to bypass this problem as it is acquired directly in the frame of reference of the patient and does not depend on any registrations. Ultrasound is a low cost and portable imaging modality that gives a real-time image of the patient, and has shown to enhance the surgical outcome [6]. Intra-operative ultrasound images gives thus an updated and reliable image of the localization of the tumor. However, the images have a limited field of view and often contain noise and artifacts that make them challenging to interpret [5].

Automatic brain tumor segmentation in intra-operative ultrasound images could facilitate the interpretation of the images and the localization of the tumor tissue, and thus help the surgeon perform a more complete resection. In addition, precise tumor

annotations in the iUS image can be used to improve the MRI-to-patient registration algorithm to correct for brain shift during surgery.

This segmentation task was the objective of the Correction of Brain Shift with Intra-Operative Ultrasound Segmentation (CuRIOUS-SEG) challenge in 2022 [30]. The training set consisted of 23 3D ultrasound images from the RESECT [29] dataset with annotations from the RESECT-SEG [2] dataset, and the test set comprised 6 annotated 3D ultrasound images. Three papers were published after this challenge, by Qayyum et al. [21], Weld et al. [27] and Sharifzadeh et al. [25]. Qayyum et al. [21] obtained the best results with an average Dice score of 0.57 obtained on the test set with a self-supervised learning-based 3DResUNet model. Moreover, all papers had difficulties with certain cases. Considering the small size of the training set, poor generalization is not unexpected. Nevertheless, the RESECT dataset, with the RESECT-SEG annotations is, to date, the only publicly available annotated dataset. Recently, Dorent et al. [9] tried a new approach for this task with a patient-specific segmentation model trained on simulated ultrasound images from labeled pre-operative MRI images from a single patient. Their approach obtain a median Dice score of 0.84-0.87 depending on the ground truth annotations when evaluated on a different 2D test set from 6 patients. In addition, they achieved better results by using the patient-specific model instead of training a general segmentation model using the RESECT dataset, where a median Dice score of 0.59-0.72 was obtained. On the other hand, this approach would only work for brain tumor segmentation before resection, and it is difficult to extend the model to include segmentation during and after resection when it is only trained on pre-resection situations. In addition, a model has to be trained for each patient which is computationally extensive and time-consuming, and may thus not be possible in a clinical context. Having a good general model that works for all patients, would be simpler and more advantageous in a clinical context. However, as discussed, the lack of a large annotated US dataset limits the performances of the current general models.

To address this issue, we investigated whether tumor annotations in pre-operative MRI images, could be used as a substitute for manual tumor delineations in ultrasound images to enlarge the training set of a deep learning model for automatic brain tumor segmentation in intra-operative ultrasound images. MRI tumor annotations are more accessible than US tumor annotation, either from published datasets[17], or by well-performing tumor segmentation software, like Raidionics [3]. Before using the MRI tumor annotations as labels, they were transformed to align with the corresponding ultrasound image space by image registration. Since non-navigated 2D ultrasound imaging is more accessible and low-cost than advanced and navigated 3D ultrasound imaging included in a technologically advanced and high-cost system [6], the 3D images and labels were sliced up to 2D images to focus on segmentation models for 2D iUS images. Training sets with only MRI tumor annotations, only US tumor annotations and with both MRI and US tumor annotations, were used to train a standardized deep learning model for medical image segmentation. All models were tested and evaluated against a separate test set with published manual tumor annotations in iUS, to compare the difference between the different label origins. In addition, the models were compared to a measured inter-observer variability obtained in this study on the

same test set. As a starting point for this novel method, only pre-resection iUS images were used with MRI tumor labels from pre-operative MRI images of patients who underwent surgery for the first time.

Data

For this project, annotated and un-annotated intra-operative ultrasound images were used. These were divided into two categories, namely US annotated data and MRI annotated data, as explained in Figure 1. The US annotated data consists of intra-operative ultrasound images with manual tumor annotations, while the MRI annotated data comprise intra-operative ultrasound images without manual tumor annotations, but with pre-operative MRI images with tumor annotations. For testing, all or parts of the US annotated data was used, depending on the experiment.

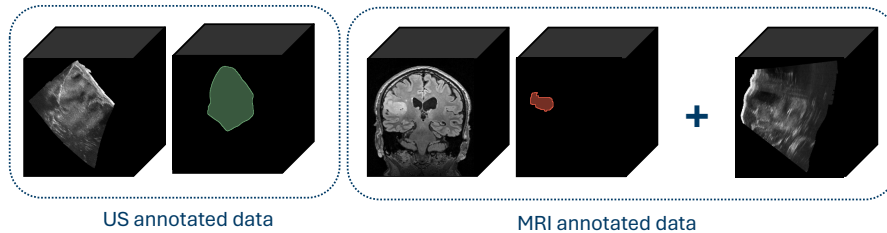


Fig. 1 The data used in this project is divided into US annotated data and MRI annotated data, where the MRI tumor annotations are used as a substitute for US tumor annotations for the MRI annotated data.

The US annotated data were obtained from 29 patients with supratentorial diffuse WHO grade 2 gliomas who underwent surgery at St. Olavs University Hospital between 2011 and 2016. Among these, 23 are published through the REtroSpective Evaluation of Cerebral Tumors (RESECT) dataset [29], where the annotations are available from the RESECT-SEG dataset [2]. Images from the remaining 6 patients were used as the test set of the CuRIOUS-SEG challenge organized in conjunction with the MICCAI 2022 conference [7], where RESECT was used as the training set. All images were 3D volumes stored as NIFTI-files. The intra-operative ultrasound images were acquired before, during and after resection, but only the images acquired before resection were used in this study giving a total of 29 ultrasound images with US tumor annotations.

The MRI annotated data consists of 180 images from the published Brain Resection Multimodal Imaging Database (ReMIND) [17], and in-house data from St. Olavs University Hospital. The ReMIND database comprises 3D iUS images and pre-operative MRI images with tumor annotations of 114 patients who underwent brain surgery at Brigham and Women’s Hospital (Boston, USA), between November 2018 and August 2022. The intra-operative ultrasound images were acquired before and after opening of the dura (pre- and post-dura) and after resection. Among the 114 patients, 92 were treated for gliomas of different WHO grades, 11 for brain metastases, and 11 for other non-tumor diseases. The database includes both re-operations and first-time surgeries.

Only the pre- and post-dura iUS images with corresponding pre-operative MRI images with tumor annotations of the patients with gliomas and metastasis who underwent surgery for the first time, were included in this study. This gave a total of 55 patients and 103 3D intra-operative ultrasound images with MRI tumor annotations, because most patients had both pre- and post-dura images.

The in-house data from St. Olavs University Hospital was collected during brain tumor resection surgeries of patients with gliomas, or with brain metastases who underwent surgeries between 2011 and 2017. The data from 2011 to 2015 was collected through several research projects on ultrasound-guided neurosurgery and later anonymized. All patients provided written informed consent at the time of data collection. The data from 2016 and 2017 were collected as a part of the Central Norway Brain Tumor Registry and Biobank, with written informed consent from all patients [4]. The iUS images were acquired in 3D and stored as NIfTI-files. Only the images acquired before resection of first-time surgeries with corresponding pre-operative contrast-enhanced T1-weighted or FLAIR MRI images were included. For cases without tumor annotation, the open-source software for automatic brain tumor segmentation in MRI images, Raidionics [3], was used. This resulted in images from 43 patients and a total of 77 3D intra-operative ultrasound images with MRI tumor annotations, since most patients have multiple pre-resection images. For all datasets combined, 29 annotated intraoperative 3D ultrasound image recordings and 180 un-annotated intraoperative 3D ultrasound image recordings with corresponding preoperative 3D MRI images from 127 patients were included in the project.

Methods

Figure 3 shows a overview of the project.

MRI-iUS registration

To use the MRI tumor annotations as labels for the ultrasound images lacking tumor annotations, the MRI tumor annotations were transferred to the corresponding ultrasound space. To do so, the pre-operative MRI images were co-registered with the corresponding ultrasound image, and the resulting transforms were applied to the corresponding MRI tumor masks. We used the rigid MRI-to-US registration algorithm proposed by Wein et al. [26] available through the medical image analysis software, ImFusion Suite (Version 2.42.2) [14] for the image registration. All registrations were visually inspected by the first author to ensure adequate alignment.

3D to 2D

To obtain 2D images from the 3D volumes, the 3D volumes were sliced in all three perpendicular directions. Only the tumor-containing slices were used for training and testing. The files were saved in the NIfTI-format. Figure 3 shows the total number of tumor-containing slices and the number of slices as a function of tumor area, for both the US annotated data and for the MRI annotated data.

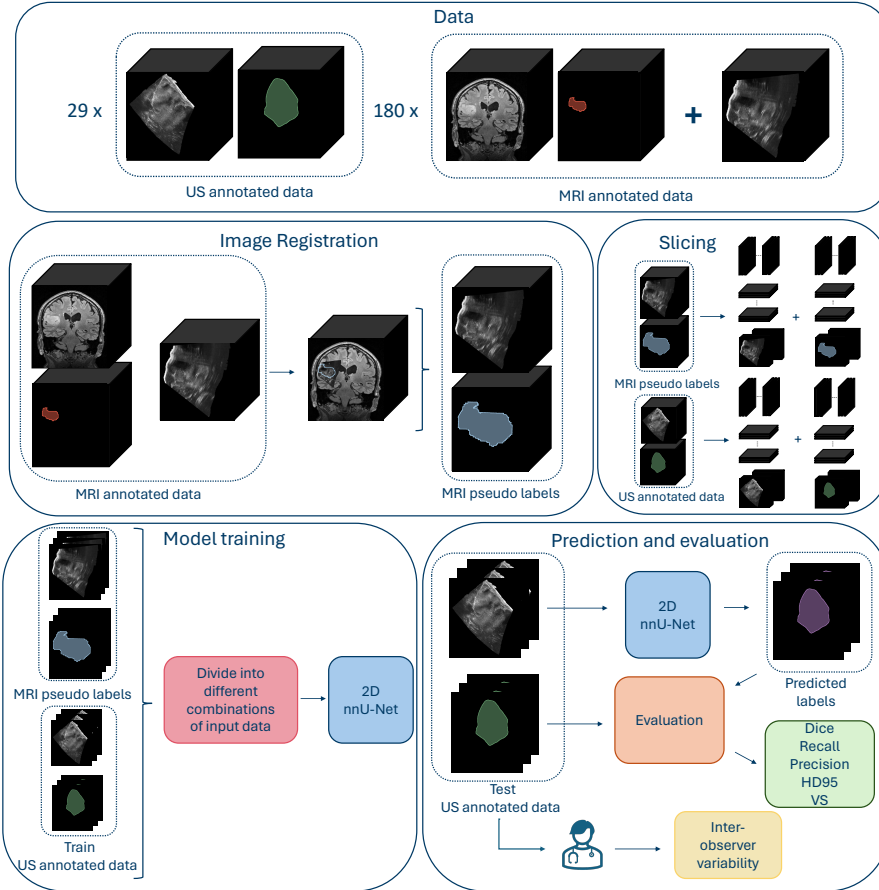


Fig. 2 Overview over the project to investigate if MRI tumor annotations can be used as US tumor annotations to train a segmentation model for intra-operative ultrasound images. ImFusion Suite [14] was used for the image registration.

Model pre-processing, training and post-processing

The open-source nnU-Net framework [15] was chosen in this study because it is a standardized and self-configuring deep learning framework where optimal pre-processing, hyper-parameters and post-processing are determined based on the given dataset. In addition, the framework has shown state-of-the-art performance within many biomedical image segmentation tasks [15]. The 2D configuration of U-Net was used with a *nnU-NetTrainer* with more data augmentation, called *nnUNetTrainerDA5*. All models were trained with five-fold cross-validation with early stopping with a patience of 30 epochs. To avoid information leaks, the fold splitting was done so that all 2D slices from one patient were kept in the same fold, and the patients were split randomly over the five folds. The pre-processing, model network and post-processing proposed by the framework for each dataset, were used. For training, an Intel Core Processor (Broadwell, no TSX, IBRS) CPU with 16 cores, 64GB of RAM, Tesla V100S (32GB)

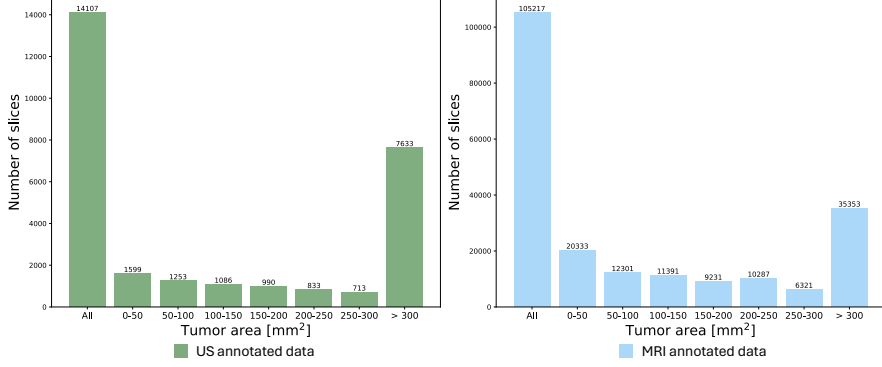


Fig. 3 The number of tumor-containing 2D slices for the US annotated and MRI annotated data, and the number of slices in different tumor area ranges.

dedicated GPU and a regular hard-drive was used. The nnU-Net framework v.2.2 was used with Python 3.8 and PyTorch v.2.2.0 [20].

Experiments

MRI annotated data: Comparison of different tumor area cut-off values

In this experiment, we used the intra-operative ultrasound images with the MRI pseudo labels obtained from the MRI annotated data explained in Figure 1. Since the images were obtained from slicing 3D volumes, the 2D slices contains tumors with a vast variability in tumor areas as seen in Figure 3. Slices from the edges of the tumor volumes are particularly small, and there is a higher risk of mismatch between the MRI pseudo label and the tumor in the iUS due to inaccurate image registration, compared to slices in the middle of the tumor volume with a larger tumor area. This experiment therefore studied different tumor area cut-off values in the MRI annotated data, to investigate the effect of excluding small and possibly poor aligned tumor labels that could be a source of noise rather than a valuable contribution to the training data. In addition, segmentation of small structures is a well-known problem in deep learning segmentation tasks, and excluding smaller structures, even with correct labels, could improve the models.

Nine models were trained in this experiment with different tumor area cut-off values measured in square millimeters. Figure 4 shows the model names and the number of training samples for each of these models. The first part of the model name is based on the label origin, thus "MRI" for this experiment. The second part of the name shows the tumor area cut-off value in square millimeters. Thus the MRI₀ model is trained on all slices with a tumor larger than 0 mm², MRI₅ on slices with a tumor area larger than 5 mm² and so on up to MRI₃₀₀ which is trained on slices with a tumor area larger than 300 mm². All models were tested on all tumor-containing slices of the 29 3D volumes of the US annotated data.

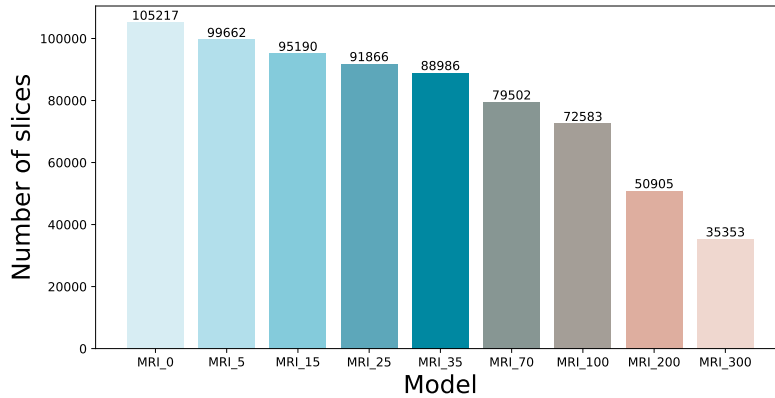


Fig. 4 The number of training samples for each model trained with MRI annotated data with different tumor area cut-off values.

MRI and US annotated data: Comparison between MRI labels, US labels and manual annotations

This experiment aimed to evaluate whether MRI tumor annotations can be used as a substitute for US tumor annotations to train a brain tumor segmentation model for ultrasound images. To do so, the MRI_200 model was compared to US_200, a model trained on only US annotated data, and MRI+US_200, a model trained on both US and MRI annotated data. In addition, the predictions of the deep learning models were compared to manual annotations validated by an expert neuro-surgeon for this project on the same test set. The US annotated data was split into a training and test set, where the 23 patients from RESECT were used for training and the 6 patients from the test set of the CuRIOUS-SEG challenge were used for testing of all models to ensure a fair comparison. Based on the results from the first experiments, 8 3D images from the MRI annotated data were excluded from the training set of the MRI+US_200 model due to poor image quality. To ensure a reasonable comparison between the models, all models were trained using nnU-Net with the same tumor area cut-off of 200 mm². This was chosen based on the results from the first experiment. The models are available here: https://github.com/mathildefaanes/us_brain_tumor_segmentation/tree/main.

Inter-observer variability

The inter-observer variability of manual intra-operative ultrasound segmentation was measured between two expert annotators, to assess the difficulty of the task. To do so, the first author manually annotated 3D images from the same 6 patients from the test set of CuRIOUS-SEG, which was also used as test set in the second experiment in this project, using 3D Slicer (Version 5.2.2) [11]. The annotations were adjusted and validated by an experienced neurosurgeon (OS) before they were sliced to 2D and compared against the sliced published ground truth segmentation masks. In the following, "Annotator" is referring to the results from this.

Evaluation and validation

To evaluate different aspects of the pixel-wise segmentation performance of each model, average Dice score, precision, recall and false negative rate (FNR) were computed between the published ground truth masks and the binary prediction masks on the test set for each experiment. Since the number of training samples changed for every model, a separate test set was used to ensure a fair comparison on unseen data. In addition, the percentage of positive predictions (PP) are calculated image-wise.

Results

MRI annotated data: Comparison of different tumor area cut-off values

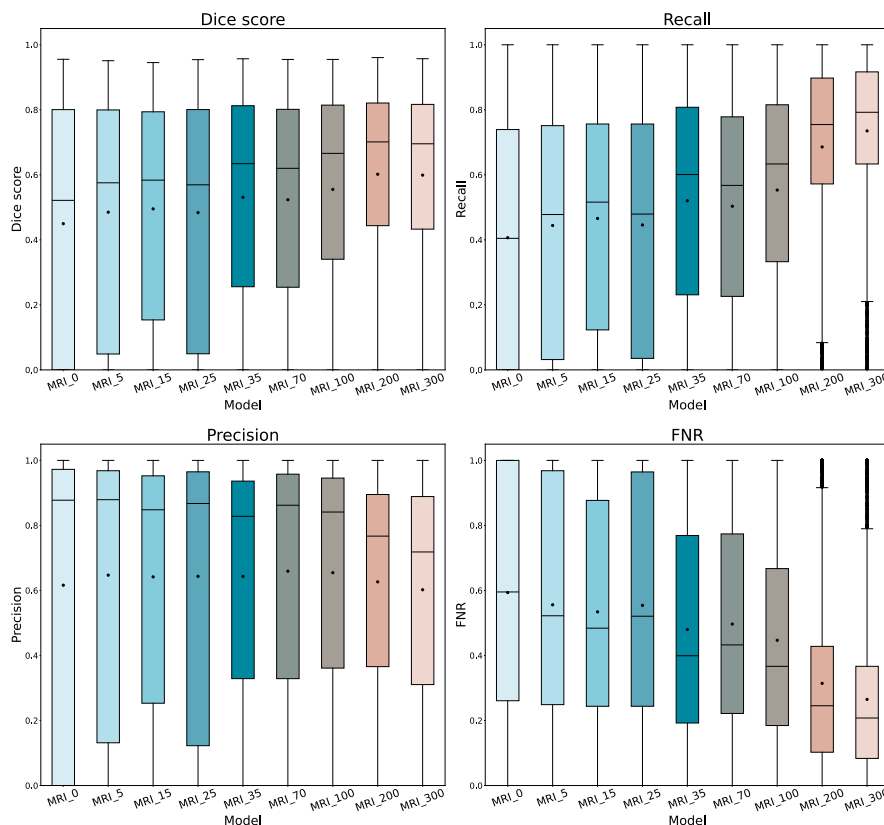


Fig. 5 Comparison of Dice score, recall, precision and false negative rate (FNR) for the 9 models trained with different tumor area cut-off values, where MRI_0 is trained using all tumor-containing slices and MRI_5 to MRI_300 are trained with slices with a tumor area larger than 5 mm^2 up to 300 mm^2 , respectively. Average values are represented by dots and median values are represented by lines.

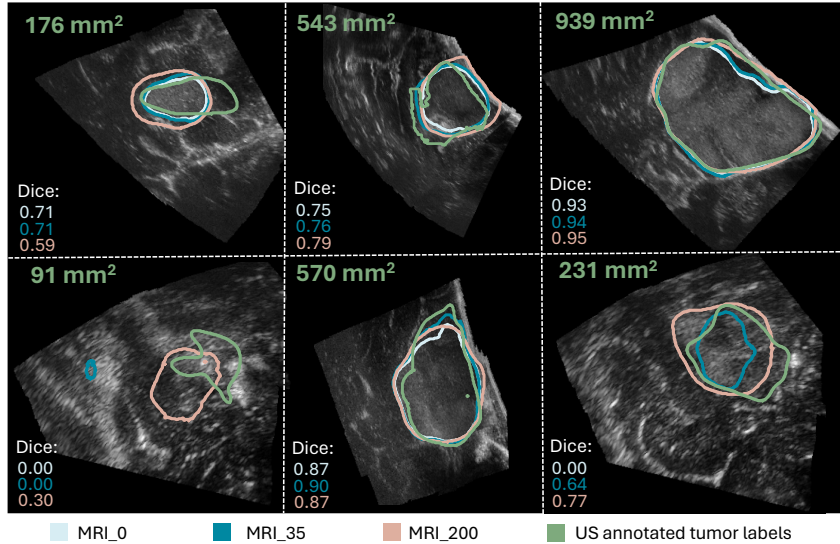


Fig. 6 Comparison of the segmentation between the ground truth (in green), the MRI.0 model (in light blue), the MRI.35 model (in blue), and the MRI.200 model (in beige). The ground truth tumor area and Dice scores are also shown for each case.

Table 1 The average Dice score with standard deviation for the nine MRI annotated data models calculated for the test 2D slices in different tumor area intervals; between 0-35 mm², 35-200 mm² and above 200 mm², and on the total amount of test slices. The percentage of positive predictions are also shown for the total test set.

Model	Tumor area ranges [mm ²]			Total	PP
	0-35	35-200	> 200		
MRI.0	0.03±0.10	0.20±0.28	0.61±0.30	0.45±0.36	72.9 %
MRI.5	0.05±0.13	0.26±0.30	0.63±0.27	0.49±0.34	79.2 %
MRI.15	0.06±0.13	0.28±0.29	0.64±0.25	0.50±0.33	84.6 %
MRI.25	0.05±0.13	0.26±0.30	0.63±0.27	0.48±0.34	78.9 %
MRI.35	0.07±0.15	0.31±0.30	0.68±0.23	0.53±0.32	87.6 %
MRI.70	0.06±0.13	0.32±0.30	0.67±0.23	0.52±0.32	86.9 %
MRI.100	0.07±0.13	0.34±0.29	0.70±0.21	0.56±0.31	90.0 %
MRI.200	0.07±0.09	0.40±0.25	0.75±0.15	0.60±0.28	98.6 %
MRI.300	0.06±0.07	0.38±0.21	0.76±0.13	0.60±0.27	99.8 %

Figure 5 shows a comparison of the evaluation metrics Dice score, recall, precision, and FNR obtained on all 29 US annotated images for the nine models trained with different tumor area cut-off values, represented by box plots. Figure 6 shows examples of predicted segmentation masks from the MRI.0, MRI.35, and MRI.200 model and the ground truth for test cases with different tumor areas, represented with the same colors as in the box plots. The Dice scores and ground truth tumor areas are also shown for each case.

Table 1 shows the average Dice score and standard deviation for different tumor area ranges of the test set for the models. In addition, it shows the percentage of positive predictions among the whole test set for each model.

MRI and US annotated data: Comparison between MRI labels, US labels and inter-observer variability

Figure 7 shows a comparison of the evaluation metrics Dice, recall, precision, and FNR, represented by box plots, for the MRI_200 model, MRI+US_200 model, US_200 model, and the Annotator. The scores were obtained on the test set of the 6 patients from the CuRIOUS-SEG challenge. The average and median Dice scores are 0.60 and 0.70 for MRI_200, 0.62 and 0.74 for MRI+US_200, 0.59 and 0.69 for US_200 and 0.67 and 0.76 for the annotator, respectively.

Figure 8 shows examples of segmentation masks from the models and the Annotator, represented with the same colors as in the box plots, and the ground truth for test slices with different tumor areas.

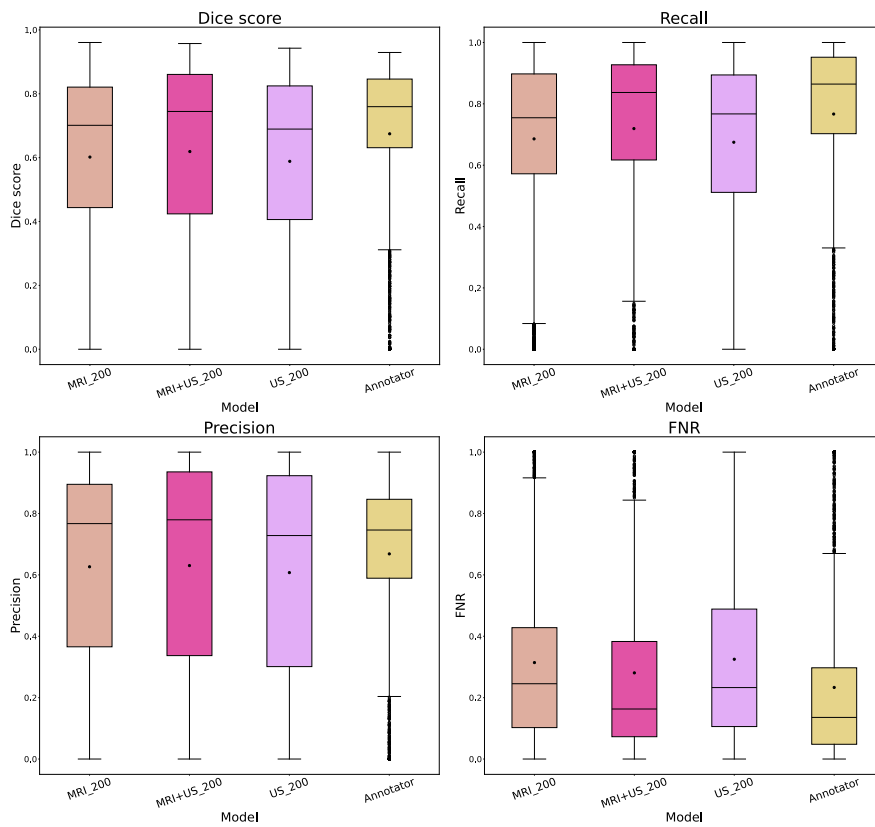


Fig. 7 Comparison of Dice score, recall, precision and false negative rate (FNR) for the MRI_200, MRI+US_200, and US_200 models, and for the Annotator.

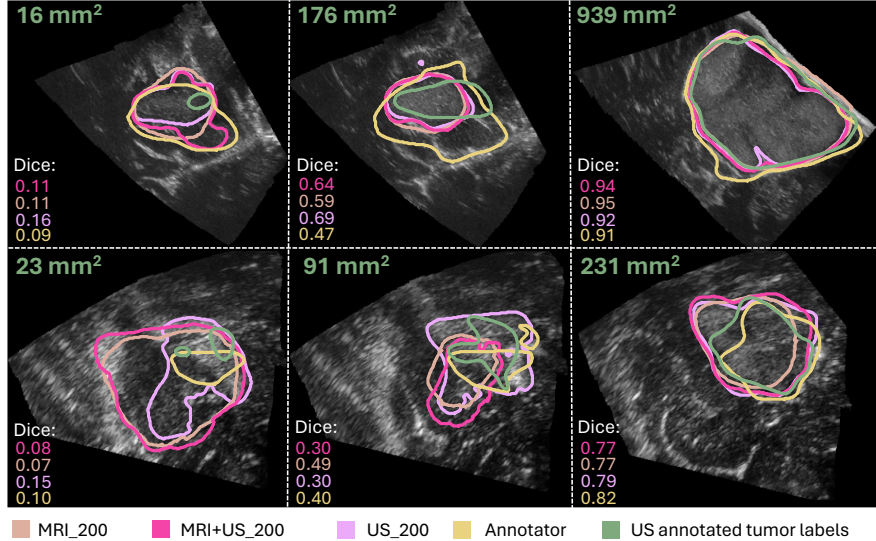


Fig. 8 Comparison of the segmentations masks from the ground truth (in green), the annotator (in yellow), the MRI_200 model (in beige), the MRI+US_200 model (in pink), and the US_200 model (in purple). The ground truth tumor area and Dice scores are also shown for each case.

Table 2 shows the average Dice score and standard deviation for different tumor area ranges of the test set, and for the total test set. In addition, it shows the percentage of positive predicted cases of the test set.

Table 2 The average Dice score with standard deviation for the MRI_200, the US_200 and the MRI+US_200 model and the annotator, calculated for the test slices in different tumor area ranges; between 0-35 mm^2 , 35-200 mm^2 and above 200 mm^2 , and on all test slices. It also shows the percentage of positive predicted cases.

Model	Tumor area ranges [mm^2]			Total	PP
	0-35	35-200	> 200		
MRI_200	0.06±0.09	0.33±0.27	0.79±0.15	0.58±0.32	96.6 %
MRI+US_200	0.08±0.10	0.40±0.27	0.81±0.12	0.62±0.31	99.0 %
US_200	0.08±0.10	0.37±0.22	0.77±0.12	0.59±0.29	100 %
Annotator	0.20±0.23	0.61±0.26	0.77±0.14	0.67±0.25	95.2 %

Discussion

This paper studied whether manual and time-consuming US tumor annotations can be replaced by MRI tumor annotations to expand the training set for an automatic brain tumor segmentation model for 2D intra-operative ultrasound images. The nnU-Net framework was used to study this by training models with different training datasets and different label origins. First, the models were trained using only registered MRI

tumor annotations as labels with different tumor area cut-off values to find the best configuration of the training data. The best performing model was compared to models trained with only US annotated tumors and both US and MRI annotated tumors, and to expert-validated manual annotations, to evaluate the use of MRI tumor annotations.

The results from the first experiment indicate that the largest difference between the models trained with different tumor area cut-off values, was their ability to detect the tumor, not segmentation performance. The MRI_200 model and MRI_300 model found a tumor in 98.6 % and 99.8 % of the test slices, respectively, while the number of predicted positive cases decreased for decreasing tumor area cut-off values to 73 % for the MRI_0 model. This is illustrated in Figure 6, which shows that the segmentation masks are similar, and that the MRI_0 and MRI_35 model fail to detect tumor in some cases. This difference in the number of predicted positive cases explains why the interquartile range shrinks and that the scores generally improve with higher tumor area cut-off values in the box plots in Figure 5 because there are less cases with empty prediction masks for increasing tumor area cut-off values. In addition, Figure 5 shows that the FNR and thus the number of false negative pixels decreases rapidly with increasing tumor area cut-off values, which also indicates that the models with higher tumor area cut-off values are better at finding tumor pixels. This also explains why the recall improves while the average precision is stable with increasing tumor area cut-off values. The reason why the median precision is higher for lower tumor area cut-off values is because false negatives are not included in the calculation of precision, and the precision scores can be high with a low true positive number and high false negative number.

The box plots also show a great difference in the median and average values, indicating a large difference in the performance for each test case, where a worse average score than median score indicates that some test cases are particularly difficult to segment. Table 1 shows that for all models, there is a large difference in the average Dice score depending on the tumor area of the test cases. It is ranging from 0.03 to 0.07 for test cases with a tumor area between 0 to 35 mm², to 0.61 to 0.76 mm² for tumors larger than 200 mm². This shows that it is the cases with a small tumor area that are particularly difficult for the models to segment. It can also be seen that the models trained with larger tumor area cut-off values obtain better Dice scores on all the tumor area ranges in the test set, including test cases with tumor areas smaller than what they have been trained on.

A possible explanation for the improvement in model performance when excluding the smallest tumors from the training set could be that the inaccuracies in the image registration has a larger impact on the smaller tumors, and including these might add more noise to the training data rather than valuable information. This illustrates that higher quality over quantity in the training data might be a good compromise in this case, as including more of the smaller tumors increases the training sample size, but decreases the performance. In addition, the segmentation task itself could be more challenging for smaller tumors because the slices with smaller tumor areas are often from the tumor border which is infiltrating healthy tissue, and could thus give a poorer contrast in the ultrasound images than the larger tumors areas. This

can be seen in Figure 6. Additionally, segmentation of small structures is a well-known challenge in medical image segmentation. The amount of tumor pixels are very low compared to background pixels, giving a high class-imbalance. Furthermore, Dice score, which is used in the loss function of nnU-Net combined with cross-entropy, is highly sensitive to errors in small structures [22], and including these in the training could be disadvantageous for the network update.

Regarding the optimal tumor area cut-off value for this dataset, it seems beneficial to remove the smallest tumors from the training set because the evaluation metrics scores are better and more stable for higher tumor area cut-off values. However, it can be seen that the MRI_300 models has the lowest precision and highest recall score, which indicates that the model is over-predicting tumor tissue and that 300 mm² is a too high cut-off value. From the Dice score box plot and from Table 1 it can be seen that the Dice scores improve until a cut-off value at 200 mm², where it stagnates. A tumor area cut-off value around 200 mm² seems thus to give the best and most stable results and was chosen as cut-off value for the comparison between label types in the second experiment.

When evaluating the use of MRI labels, the results from the second experiment showed similar performance on all evaluation metrics for a model trained with only MRI annotated tumors compared to a model trained with only US annotated tumors, or both MRI and US annotated tumors, as seen in Figure 7. This indicates that MRI annotated tumors can be used as labels for this purpose. In addition, the figure and Table 2 showed that using both US and MRI tumor annotations achieved the best evaluation metric scores, with an average Dice score of 0.62 on the entire test set, compared to 0.58 and 0.59 for the MRI_200 and US_200 model, respectively. This indicates that it is beneficial to combine both label types to create a larger dataset. However, the difference is relatively small, even though the models are trained on an around 8 times larger dataset. From Table 2, it can be seen that the models in this experiment also have poor prediction results on the small tumors. Figure 7 illustrates this, where it can be seen that the segmentation masks are closer to the ground truth for larger tumors. Segmentation of the small tumor seems to be a limiting factor for improving the scores further.

From Figure 7 it can also be seen that for some cases, there is a large difference between the ground truth segmentation and the Annotator, indicating that there can be a large discrepancy in how different experts annotate the tumor. From Table 2, it can be seen that the Annotator obtained a Dice score of 0.67 which is far from a 100 % overlap with the ground truth segmentations. This underscores that brain tumor segmentation in ultrasound images is a challenging task, also for experienced neurosurgeons. The goal for the deep learning models is thus not to achieve a Dice score of 1, but rather a Dice score similar to the inter-observer variability score. The same applies for the other evaluation metrics.

When comparing the deep learning models to the Annotator, the results showed that the annotator achieved superior scores for all metrics on the entire test set. The average Dice score on the test set was 0.67, compared to 0.62, 0.59 and 0.58 for the MRI+US_200, US_200 and MRI_200 model. Nevertheless, Table 2 showed that the Dice scores obtained on the larger tumors (> 200 mm²) were equal to or slightly lower

than the scores achieved by the deep learning models, indicating that the performances of the models on larger tumors are on an expert-level. On the contrary, there is a large gap in the Dice scores obtained on the smaller tumors (0-35 mm² and 35-200 mm²) in the test set between the annotator and the deep learning model. Again, this indicates that the smaller tumors are a limiting factor for the deep learning models.

Compared to previous work, Qayyum et al. [21] obtained an average Dice score of 0.57 on the same test set, but in 3D. Even though this is not directly comparable, it indicates that our approach achieves comparable or better results, and supports the usage of MRI tumor annotations. The patient-specific approach of Dorent et al. [9], achieved better results with a median Dice score of 0.84-0.87, compared to 0.74 for the MRI+US_200 model. However, this is as expected since they are training models on each patient, thus overfitting to the training data. Nevertheless, they are also using MRI labels in their method when training the patient-specific models using simulated ultrasound images from MRI, which also support the use of MRI tumor labels as a replacement for US tumor annotations.

In spite of promising reported performances using MRI annotated tumors as labels, the task of intra-operative brain tumor segmentation is not accomplished. A limiting factor in this study is that the comparison between the models, previous work and the external annotator is only done on images from 6 patients with WHO grade 2 gliomas. As reported in [10], the models performance on the test set is highly sensitive to the test samples depending on the tumor sizes and tumor contrast. A larger test set with more tumor types annotated by multiple experts should be acquired and used to evaluate models before a possible clinical implementation.

In addition, even though the performance for larger tumors showed promising results, the results are poor for the smaller tumors. The small structures seem to be a limiting factor both when including them in the training and in the test set. This should be the focus of future work and is crucial for extending the model for segmentation during and after resection, where the tumors are smaller. Using MRI labels from post-operative MRI with corresponding iUS images and using pre-operative MRI images from patients who has undergone previous surgery with corresponding iUS images can be included, in order to increase the number of smaller tumors in the training set. An affine or non-linear registration method could be tested for the MRI labels to match the real tumor better for the slices with the smaller tumor areas. In addition, a different loss function that is more suitable for smaller structures could improve the results. Also, a fundamentally different deep learning network could be tested like a vision transformer network, or a pre-trained network on medical images like MedNet [1] or foundation models like USFM [16], to evaluate if this improves the scores for the smaller structures. Other strategies than semantic segmentation could also be investigated for the smaller structures, such as bounding boxes proposed by Weld et. al [28].

Conclusion

In this study, the use of MRI tumor annotations as a substitute for intra-operative ultrasound images lacking tumor annotations to enlarge the training set for an automatic brain tumor segmentation model for 2D intra-operative ultrasound images, was investigated. The results showed no difference between a model trained with only ultrasound annotated labels and a model trained with only MRI annotated labels. In addition, a model that was trained using both label types obtained the best evaluation scores with an average Dice score of 0.62, compared to 0.67 for expert annotations. This indicates that the MRI tumor annotations can be used as a substitute. For tumors larger than 200 mm², our models achieved similar performance as the external expert annotator. However, the performance on smaller tumors is poor and limits possible clinical implementation.

Declarations

Funding

This project was partially funded by the National research centre for minimally invasive and image-guided diagnostics and therapy (MiDT), Trondheim, Norway.

Competing Interests

All the authors declare that they have no conflict of interest.

Ethical approval

This study has been approved and performed in accordance with ethical standards.

Informed consent

Informed consent was obtained from all participants in this study.

References

- [1] Alzubaidi L, Santamaría J, Manoufali M, et al (2021) MedNet: Pre-trained Convolutional Neural Network Model for the Medical Imaging Tasks. <https://doi.org/10.48550/arXiv.2110.06512>, arXiv:2110.06512 [cs]
- [2] Behboodi B, Carton FX, Chabanas M, et al (2022) RESECT-SEG: Open access annotations of intra-operative brain tumor ultrasound images. <https://doi.org/10.48550/arXiv.2207.07494>, arXiv:2207.07494 [physics]
- [3] Bouget D, Alsinan D, Gaitan V, et al (2023) Raidionics: an open software for pre- and postoperative central nervous system tumor segmentation and standardized reporting. *Scientific Reports* 13(1):15570. <https://doi.org/10.1038/s41598-023-42048-7>, URL <https://www.nature.com/articles/s41598-023-42048-7>, number: 1 Publisher: Nature Publishing Group

- [4] Cancer Registry of Norway (2023) Norwegian registry of brain and spinal cord tumours. URL <https://www.kreftregisteret.no/en/The-Registries/clinical-registries/Quality-registry-for-brain-tumours/>
- [5] Carton FX (2021) Image segmentation and registration using machine learning for brain shift compensation in image-guided neurosurgery. phdthesis, Université Grenoble Alpes [2020-....] ; Vanderbilt university (Nashville, Tennessee)
- [6] Cepeda S, García-García S, Arrese I, et al (2024) Non-navigated 2D intraoperative ultrasound: An unsophisticated surgical tool to achieve high standards of care in glioma surgery. *Journal of Neuro-Oncology* 167(3):387–396. <https://doi.org/10.1007/s11060-024-04614-5>
- [7] CuRIOUS 2022 (2022) Brain shift with Intraoperative Ultrasound - Segmentation tasks - Grand Challenge. URL <https://curious2022.grand-challenge.org/>
- [8] Delgado-López PD, Corrales-García EM, Martino J, et al (2017) Diffuse low-grade glioma: a review on the new molecular classification, natural history and current management strategies. *Clinical and Translational Oncology* 19(8):931–944. <https://doi.org/10.1007/s12094-017-1631-4>, URL <https://doi.org/10.1007/s12094-017-1631-4>
- [9] Dorent R, Torio E, Haouchine N, et al (2024) Patient-specific real-time segmentation in trackerless brain ultrasound. *Medical Image Computing and Computer Assisted Intervention – MICCAI 2024*
- [10] Faanes MG (2024) Automatic brain tumor segmentation in intra-operative ultrasound images using deep learning. Master’s thesis, NTNU, URL <https://ntnuopen.ntnu.no/ntnu-xmlui/handle/11250/3154957>
- [11] Fedorov A, Beichel R, Kalpathy-Cramer J, et al (2012) 3D Slicer as an image computing platform for the Quantitative Imaging Network. *Magnetic Resonance Imaging* 30(9):1323–1341. <https://doi.org/10.1016/j.mri.2012.05.001>
- [12] Gerard IJ, Kersten-Oertel M, Petrecca K, et al (2017) Brain shift in neuronavigation of brain tumors: A review. *Medical Image Analysis* 35:403–420. <https://doi.org/10.1016/j.media.2016.08.007>
- [13] Hentschel SJ, Sawaya R (2003) Optimizing Outcomes with Maximal Surgical Resection of Malignant Gliomas. *Cancer Control* 10(2):109–114. <https://doi.org/10.1177/107327480301000202>, URL <https://doi.org/10.1177/107327480301000202>, publisher: SAGE Publications Inc
- [14] ImFusion (2018) ImFusion - ImFusion Suite. URL <https://www.imfusion.com/products/imfusion-suite>

- [15] Isensee F, Jäger PF, Full PM, et al (2021) nnU-Net for Brain Tumor Segmentation. In: Crimi A, Bakas S (eds) Brainlesion: Glioma, Multiple Sclerosis, Stroke and Traumatic Brain Injuries. Springer International Publishing, Cham, Lecture Notes in Computer Science, pp 118–132, https://doi.org/10.1007/978-3-030-72087-2_11
- [16] Jiao J, Zhou J, Li X, et al (2024) USFM: A universal ultrasound foundation model generalized to tasks and organs towards label efficient image analysis. *Medical Image Analysis* 96:103202. <https://doi.org/10.1016/j.media.2024.103202>, URL <https://www.sciencedirect.com/science/article/pii/S1361841524001270>
- [17] Juvekar P, Dorent R, Kogl F, et al (2023) ReMIND: The Brain Resection Multimodal Imaging Database. <https://doi.org/10.1101/2023.09.14.23295596>, URL <https://www.medrxiv.org/content/10.1101/2023.09.14.23295596v1>, pages: 2023.09.14.23295596
- [18] Kheirollahi M, Dashti S, Khalaj Z, et al (2015) Brain tumors: Special characters for research and banking. *Advanced Biomedical Research* 4:4. <https://doi.org/10.4103/2277-9175.148261>, URL <https://www.ncbi.nlm.nih.gov/pmc/articles/PMC4300589/>
- [19] Louis DN, Perry A, Wesseling P, et al (2021) The 2021 WHO Classification of Tumors of the Central Nervous System: a summary. *Neuro-Oncology* 23(8):1231–1251. <https://doi.org/10.1093/neuonc/noab106>, URL <https://www.ncbi.nlm.nih.gov/pmc/articles/PMC8328013/>
- [20] Paszke A, Gross S, Massa F, et al (2019) PyTorch: An Imperative Style, High-Performance Deep Learning Library. In: *Advances in Neural Information Processing Systems*, vol 32. Curran Associates, Inc.
- [21] Qayyum A, Mazher M, Niederer S, et al (2023) Segmentation of Intra-operative Ultrasound Using Self-supervised Learning Based 3D-ResUnet Model with Deep Supervision. In: Xiao Y, Yang G, Song S (eds) *Lesion Segmentation in Surgical and Diagnostic Applications*. Springer Nature Switzerland, Cham, Lecture Notes in Computer Science, pp 55–62, https://doi.org/10.1007/978-3-031-27324-7_7
- [22] Reinke A, Tizabi MD, Sudre CH, et al (2023) Common Limitations of Image Processing Metrics: A Picture Story. <https://doi.org/10.48550/arXiv.2104.05642>, URL <http://arxiv.org/abs/2104.05642>, arXiv:2104.05642 [cs, eess]
- [23] Sanai N, Berger MS (2008) GLIOMA EXTENT OF RESECTION AND ITS IMPACT ON PATIENT OUTCOME. *Neurosurgery* 62(4):753. <https://doi.org/10.1227/01.neu.0000318159.21731.cf>, URL https://journals.lww.com/neurosurgery/abstract/2008/04000/glioma_extent_of_resection_and_its_impact_on.10.aspx

- [24] Sastry R, Bi WL, Pieper S, et al (2017) Applications of Ultrasound in the Resection of Brain Tumors. *Journal of Neuroimaging* 27(1):5–15. <https://doi.org/10.1111/jon.12382>, URL <https://onlinelibrary.wiley.com/doi/abs/10.1111/jon.12382>
- [25] Sharifzadeh M, Benali H, Rivaz H (2023) Segmentation of Intraoperative 3D Ultrasound Images Using a Pyramidal Blur-Pooled 2D U-Net. In: Xiao Y, Yang G, Song S (eds) *Lesion Segmentation in Surgical and Diagnostic Applications*. Springer Nature Switzerland, Cham, *Lecture Notes in Computer Science*, pp 69–75, https://doi.org/10.1007/978-3-031-27324-7_9
- [26] Wein W, Brunke S, Khamene A, et al (2008) Automatic CT-ultrasound registration for diagnostic imaging and image-guided intervention. *Medical Image Analysis* 12(5):577–585. <https://doi.org/10.1016/j.media.2008.06.006>, URL <https://www.sciencedirect.com/science/article/pii/S1361841508000637>
- [27] Weld A, Agrawal A, Giannarou S (2023) Ultrasound Segmentation Using a 2D UNet with Bayesian Volumetric Support. In: Xiao Y, Yang G, Song S (eds) *Lesion Segmentation in Surgical and Diagnostic Applications*. Springer Nature Switzerland, Cham, *Lecture Notes in Computer Science*, pp 63–68, https://doi.org/10.1007/978-3-031-27324-7_8
- [28] Weld A, Dixon L, Anichini G, et al (2024) Challenges with segmenting intraoperative ultrasound for brain tumours. *Acta Neurochirurgica* 166(1):317. <https://doi.org/10.1007/s00701-024-06179-8>, URL <https://doi.org/10.1007/s00701-024-06179-8>
- [29] Xiao Y, Fortin M, Unsgård G, et al (2017) REtroSpective Evaluation of Cerebral Tumors (RESECT): A clinical database of pre-operative MRI and intra-operative ultrasound in low-grade glioma surgeries. *Medical Physics* 44(7):3875–3882. <https://doi.org/10.1002/mp.12268>
- [30] Xiao Y, Yang G, Song S (eds) (2023) *Lesion Segmentation in Surgical and Diagnostic Applications: MICCAI 2022 Challenges, CuRIOUS 2022, KiPA 2022 and MELA 2022, Held in Conjunction with MICCAI 2022, Singapore, September 18–22, 2022, Proceedings, Lecture Notes in Computer Science, vol 13648*. Springer Nature Switzerland, Cham, <https://doi.org/10.1007/978-3-031-27324-7>